Matykina, E.; Arrabal, R.; Pardo, A.; Mohedano, M.; Mingo, B.;
Rodriguez, I.; Gonzalez, J.:

Energy-efficient PEO process of aluminium alloys

In: Materials Letters (2014) Elsevier

DOI: 10.1016/j.matlet.2014.04.077

Energy-efficient PEO process of aluminium alloys

E. Matykina*[1], R. Arrabal[1], A. Pardo[1], M. Mohedano[2], B. Mingo[1], I. Rodríguez[1], J. González[1]

[1] *Departamento de Ciencia de Materiales, Facultad de Ciencias Químicas, Universidad Complutense, 28040, Madrid, Spain*

[2] *Helmholtz Zentrum Geesthacht, Magnesium Innovation Centre, Institute of Materials Research, Max-Planck-Str. 1, D-21502 Geesthacht, Germany*

*corresponding author: ematykin@ucm.es

Abstract

The influence of pre-anodizing in sulphuric and phosphoric acids on energy efficiency of voltage-controlled PEO process of three commercial wrought and cast aluminium alloys (AA1050, AA6082 and A356) has been investigated. The precursor anodic porous films enable up to 57% energy savings during PEO and produce ~35-40% increase of the coating microhardness compared with direct PEO. Total specific energy consumption values of 2.5-2.7 kW h m^{-2} μm^{-1} and 3.1-3.8 kW h m^{-2} μm^{-1} were achieved using phosphoric and sulphuric acid-formed precursors, respectively.

Keywords: metals and alloys; thick films; oxidation.

1. Introduction

Plasma electrolytic oxidation (PEO) produces multi-functional ceramic coatings on strategically important lightweight alloys such as Al, Ti and Mg [1, 2] with enhanced corrosion, wear, thermo-optical, dielectric and thermal barrier properties [3-8]. PEO can also be used as a base for topcoat paints and to create composite coatings [9, 10].

Typical PEO coatings on aluminium alloys are 50-100 μm-thick; they comprise a ~300 nm thick barrier layer adjacent to the substrate, an ultrahard (1000-2000 HV) intermediate layer with microcracks and submicrometer-size pores, and an outer porous layer that usually constitutes up to about 30% of the coating thickness [11, 12]. Corrosion resistance is mainly attributed to the barrier layer [13], whereas the intermediate layer provides the main thermomechanical and tribological functionality of the coating [14].

The PEO process lasts 10-60 min, depending upon the substrate material, current regime and desired coating thickness, and is characterized by the generation of numerous short-lived microdischarges caused by dielectric breakdown of oxide film at high voltages. At the location of microdischarges, rapid heating and cooling promotes the formation of high-temperature phases (*e.g.* α-Al_2O_3) desirable for tribological applications [3]. Coatings with a denser intermediate layer are formed under ac and bi-polar conditions due to the establishment of a particular microarc regime that is commonly referred to as "soft sparking" [15, 16]. The transition to this regime commences after a sufficient thickness of the coating has been achieved (15-20 μm) and is characterized by contraction of the positive column of the microarc discharge, low acoustic emission and increased emissions from bound-free electron transitions in the optical spectrum of the microdischarges [11, 17, 18]. In current-controlled mode, a voltage drop is also observed during the transition [16].

So far, PEO technology has only been exploited for some highly demanding and niche applications due to its relatively high cost associated with high energy consumption and low coating efficiency [19]. Current densities and voltages are typically between 10-60 A/dm^2 and 200-400 V (rms), respectively, and the efficiency of conversion of the anodic charge into the final coating material may be as low as 20%, due to gas generation and dissolution processes [20, 21]. Therefore, the process efficiency must be improved in order to make this technology commercially viable for high-volume applications, *i.e.* automotive components.

Recently, use of conventional anodizing as a pre-treatment [11, 16, 22] has been demonstrated to promote the establishment of "soft sparking" regime in current-controlled PEO of high purity aluminium, resulting in greater coating growth rates which helps to overcome the cost limitations of the process. However, many commercial and semi-commercial PEO sources operate in voltage or power-controlled mode [1, 19], therefore there is a need to investigate the effectiveness of the precursor approach for those cases.

The present study compares the effects of pre-anodizing in sulphuric and phosphoric acids on the specific energy consumption of the voltage-controlled PEO treatment of three different commercially available aluminum alloys. Comparison with high purity aluminium is also given.

2. Materials and methods

High purity Al (99.99%), wrought alloys AA1050-H18 (wt.%: 0.07 Zn, 0.05 Mn, 0.25 Si, 0.5 Cu, 0.40 Fe, 0.05 Mg, bal. Al), AA6082-T6 (wt.%: 0.015 Zn, 0.62 Mn, 0.86 Si, 0.022 Cu, 0.25 Fe, 0.84 Mg, bal. Al) and cast alloy A356-F (wt.%: <0.001 Zn, 0.0006 Mn, 6.83 Si, 0.153 Fe, 0.366 Mg, bal. Al) with 3 cm^2 working area were degreased in isopropyl alcohol, etched in 20% NaOH during 10 s (AA6082 and A356 were additionally desmutted in concentrated HNO_3), rinsed in deionized water and dried in warm air.

The porous precursor films were formed by anodizing in sulphuric and phosphoric acid, respectively, using conditions described elsewhere [11]. PEO treatments were carried out using a voltage-controlled EAC-S2000 power supply (ET systems electronic) in an electrolyte comprising 10.5 g/L sodium silicate solution ($Na_2O(SiO_2)_x \cdot xH_2O$, ≥27% SiO_2, ρ=1.39 g/L) and 0.05 M KOH. Square waveform with a positive and negative voltage amplitudes of 490 V and -110 V, respectively, duty cycle 50%, frequency 50 Hz and a current density limit j_{rms}=500 mA/cm^2 were used. Further details on the experimental rig can be found in [11, 23].

Following a standard metallographic preparation sample cross sections were examined by scanning electron microscopy (SEM) using a JEOL JSM 6400 instrument. Coating thickness was measured using an eddy-current meter ISOSCOPE FMP10 (Fischer) equipped with FTA3.3H probe, taking an average of 10 measurements and further verified using SEM. Surface roughness was measured in five different locations using a Surtronic 25 tester (Taylor Hobson Precision, UK) and TalyProfile software applying a gaussian filter of 0.25 mm. Micro-hardness was measured in coating cross-sections using an AKASHI MVK-E3 instrument applying a 50 g load maintained during 20 s.

3. Results and Discussion

The porous precursor films with different thickness on high purity aluminium were preliminary screened and 20 μm-thick films (S20 and P20, for sulphuric and phosphoric acid-formed films, respectively) demonstrated the optimal combination of surface appearance and energy consumption of PEO. Thickening of the barrier layer in boric acid of the S20 precursors as in [11] have shown no significant benefit to the specific energy consumption, whereas in P20 it produced considerable reduction in the energy. Therefore the S20 and P20+B (porous film with thickened barrier layer) were employed for further studies using commercial alloys.

The effect of the precursors on the energy consumption compared with the direct PEO treatment can be perceived from Figures 1 (a-c). The current drop observed in each case corresponds to uniform establishment of "soft sparking" over the entire specimen surface. Such current drop is attributed here to an increased thickness and density of the coating over the entire specimen surface and consequently the higher resistance of the oxide material to mass transfer. To achieve a uniform coating thickness, the PEO process was carried on for 600 s from the moment of the current drop to termination. Over the first minutes of direct PEO, the AA1050 alloy and pure Al (not included) show an additional current drop, followed by a recovery, that is not observed in case of the AA6082 and A356 alloys. This initial drop could be explained by the formation of a barrier layer with higher impedance since the amount of secondary phases that could break the continuity of this layer is negligible. Later, with the initiation of "soft sparking", the current reached again the set limit. The geometry of the pore influences the mechanism of the discharge [11]; as a result the precursor films enabled reduction of the treatment time by 2-3 times, depending on the alloy; in general 90-100 μm-thick coatings were produced in 20-25 min (Fig. 2).

The specific energy consumption of the PEO process (E_{PEO}) was calculated by integration of the instantaneous voltage and current waveforms (Fig. 1(d)) recorded periodically (Table 1). The total energy (E_{total}) includes the energy consumed by PEO, formation of the porous film precursor and thickening of the barrier layer. The energy consumption by the two latter processes is about 2-5% of E_{PEO}. Compared with the direct PEO treatment, S20 precursor films reduced the E_{total} by 38%, 32%, 24% and 32% for pure Al, AA1050, AA6082 and A356 alloys, respectively, the E_{total} energies ranging within ~3.0-3.8 kW h m^{-2} μm^{-1}. P20+B precursor was more efficient and yielded, respectively, 57%, 51%, 39% and 52% energy reductions, compared with directly treated alloys, E_{total} corresponding to ~2.0 kW h m^{-2} μm^{-1} for pure aluminium and ~2.5-2.7 kW h m^{-2} μm^{-1} for commercial alloys. Such improvement is possibly related to the greater diameter of the pores formed in phosphoric acid (80 nm) than in sulphuric acid (20 nm) [11], however the relationship with the current drop is not obvious and requires further studies. The PEO coating growth rates on pre-anodized alloys were in general 2-3 times higher than on non-pre-anodized alloys; in all cases 3.2-4.4 μm min^{-1} growth rates were achieved (Table 1).

These values are similar or lower than those obtained in current-controlled PEO of pure aluminium [11] and considerably lower compared with the data available for different modes of PEO process of commercial aluminium alloys [19]: e.g. the specific energy consumption in technologically important silicate-phosphate electrolytes may be as high as 26.7 kW h m^{-2} μm^{-1}.

The precursor films did not in general alter the PEO coating morphology and roughness (Fig. 2), compared with non-pre-anodized materials (Table 1). However, a considerable improvement of the microhardness of the intermediate layer of the coating was achieved in AA1050 and AA6082 alloys (Fig. 3). For instance, compared with the non-pre-anodized alloy ($HV_{0.05}$ 1031), the PEO of AA6082 alloy with precursors yielded the average $HV_{0.05}$ values of 1448 and 1337 for S20 and P20+B, respectively. Enhanced microhardness is attributed to the greater amount of α-Al_2O_3 that forms under rapidly established "soft" sparking regime [12, 15]: the faster the "soft" sparking established and the longer the PEO time, the greater hardness is achieved. Silicon particles in A356 alloy and associated coating porosity result in substantially lower microhardness of these materials, ~900 $HV_{0.05}$.

4. Conclusions

- Sulphuric and phosphoric acid-formed anodic precursors allow for up to 57% reduction of the energy consumption of voltage-controlled PEO process of commercial wrought and cast aluminium alloys, compared with non-pre-anodized alloys. P20+B precursor yields lower energy consumption values (2.5-2.7 kW h m^{-2} μm^{-1}) than S20 precursor (3.1-3.8 kW h $m^{-2}\mu m^{-1}$).
- The precursors enable ~100 μm-thick coatings to be achieved in ~1500 s, compared with ~3000-4000 s for precursor-free alloys.
- The precursors lead to increase of the microhardness of PEO coatings on AA1050 and AA6082 alloys by ~35-40%, yielding in the average 1337-1468 $HV_{0.05}$.

Acknowledgements

The authors are grateful to MICINN (Spain, MAT2012-38407-C03-02) for financial support. E. Matykina is grateful to the Ramon y Cajal Programme (MICINN, Spain, RYC-2010-06749).

References

1. Yerokhin AL, Nie X, Leyland A, Matthews A, Dowey SJ. Surf Coat Technol 1999;122:73-93
2. Butyagin PI, Khokhryakov YV, Mamaev AI. Mater Lett 2003;57:1748-51
3. Curran JA, Clyne TW. Surf Coat Technol 2005;199:168-76
4. Gnedenkov SV, Khrisanfova OA, Zavidnaya AG, Sinebrukhov SL, Kovryanov AN, Scorobogatova TM et al. Surf Coat Technol 2000;123:24-28
5. Blawert C, Heitmann V, Dietzel W, Nykyforchyn HM, Klapkiv MD. Surf Coat Technol 2007;201:8709-14

6. Cheng Y, Cao J, Peng Z, Wang Q, Matykina E, Skeldon P et al. Electrochim Acta 2014;116:453-66

7. Du K, Guo X, Guo Q, Wang F, Tian Y. Mater Lett 2013;91:45-49

8. Guo H, An M, Xu S, Huo H. Mater Lett 2006;60:1538-41

9. Shoaei-Rad V, Bayati MR, Golestani-Fard F, Zargar HR, Javadpour J. Mater. Lett 2011;65:1835-38

10. Arrabal R, Mota JM, Criado A, Pardo A, Mohedano M, Matykina E. Surf Coat Technol 2012;206:4692-703

11. Matykina E, Arrabal R, Skeldon P, Thompson GE, Belenguer P. Surf Coat Technol 2010;205:1668-78

12. Yerokhin AL, Shatrov A, Samsonov V, Shashkov P, Pilkington A, Leyland A et al. Surf Coat Technol 2005;199:150-57

13. Barik RC, Wharton JA, Wood RJK, Stokes KR, Jones RL. Surf Coat Technol 2005;199:158-67

14. Curran JA, Clyne TW. Surf Coat Technol 2005;199:177-83

15. Jaspard-Mecuson F, Czerwiec T, Henrion G, Belmonte T, Dujardin L, Viola A et al. Surf Coat Technol 2007;201:8677-82

16. Matykina E, Arrabal R, Mohamed A, Skeldon P, Thompson GE. Corr Sci 2009;51:2897-905

17. Mecuson F, Czerwiec T, Belmonte T, Dujardin L, Viola A, Henrion G. Surf Coat Technol 2005;200:804-08

18. Hussein RO, Nie X, Northwood D, Yerokhin OA, Matthews A. J Phys D Appl Phys 2010;43:105203

19. Yerokhin AL, Shatrov A, Samsonov V, Shashkov P, Pilkington A, Leyland A et al. Surf Coat Technol 2005;199:150-57

20. Snizhko LO, Yerokhin AL, Gurevina NL, Patalakha VA, Matthews A. Thin Solid Films 2007;516:460-64

21. Snizhko LO, Yerokhin AL, Pilkington A, Gurevina NL, Misnyankin DO, Leyland A et al. Electrochim Acta 2004;49:2085-95

22. Matykina E, Arrabal R, Skeldon P, Thompson GE. Surf Interf Anal 2010;42:221-26

23. Mohedano M, Matykina E, Arrabal R, Pardo A, Merino MC. Dental Mater 2014;30:e28-e40

Figure Captions

Figure 1. Voltage and current-time dependencies for PEO of aluminium alloys with precursor films: (a) AA1050-H18; (b) AA6082-T6; (c) A356-F; (d) instantaneous voltage and current waveforms.

Figure 2. Backscattered electron images of the PEO coating cross-sections without precursor (a-c), and with precursors formed in sulphuric (d-f) and phosphoric (g-i) acids.

Figure 3. Microhardness of the materials with various treatments.

Table 1. Parameters of the PEO coatings obtained on three studied alloys with and without precursor films

Material	**Treatment**	**E_{PEO} (kW h m^{-2} μm^{-1})**	**E_{total} (kW h m^{-2} μm^{-1})**	**Thickness (μm)**	**Growth rate (μm min^{-1})**	**R_a (μm)**
Pure Al	PEO	4.77	4.77	98±3	1.3	4.3±0.2
	S20 + PEO	2.89	2.97	101±4	4.3	4.2±0.3
	P20+B+PEO	1.93	2.04	98±3	4.4	4.4±0.3
AA1050	PEO	5.57	5.57	82±3	1.4	3.4±0.2
	S20 + PEO	3.74	3.81	95±4	3.2	4.4±0.2
	P20+B+PEO	2.47	2.71	96±3	3.8	4.9±0.4
AA6082	PEO	4.14	4.14	88±4	2.0	4.1±0.3
	S20 + PEO	3.10	3.16	103±4	4.1	4.0±0.2
	P20+B+PEO	2.28	2.52	101±3	3.9	4.6±0.2
A356	PEO	5.28	5.28	83±4	1.0	5.9±0.3
	S20 + PEO	3.52	3.58	75±4	3.3	4.4±0.2
	P20+B+PEO	2.39	2.52	88±4	3.5	4.6±0.3

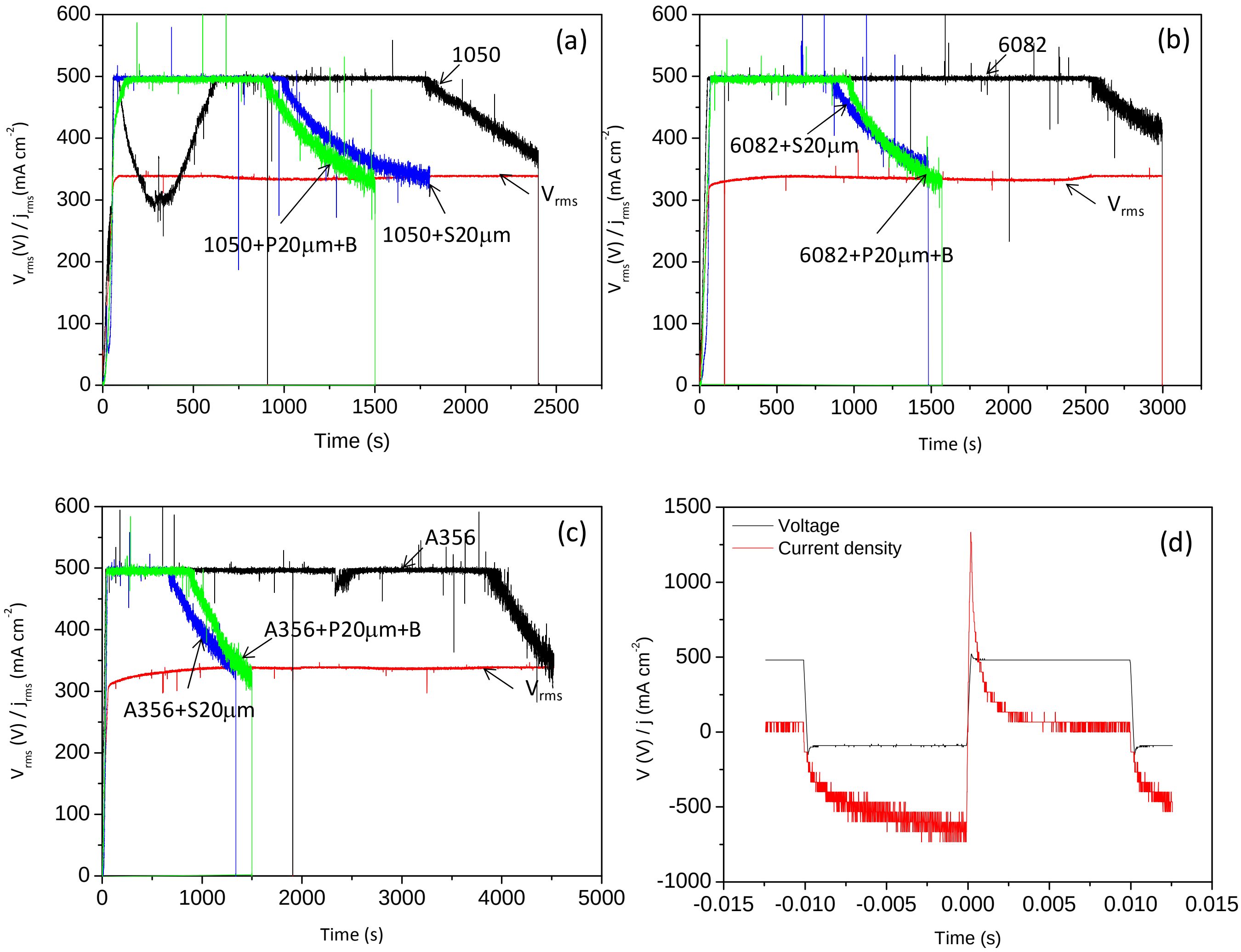

Figure 1. ***Matykina et al.***

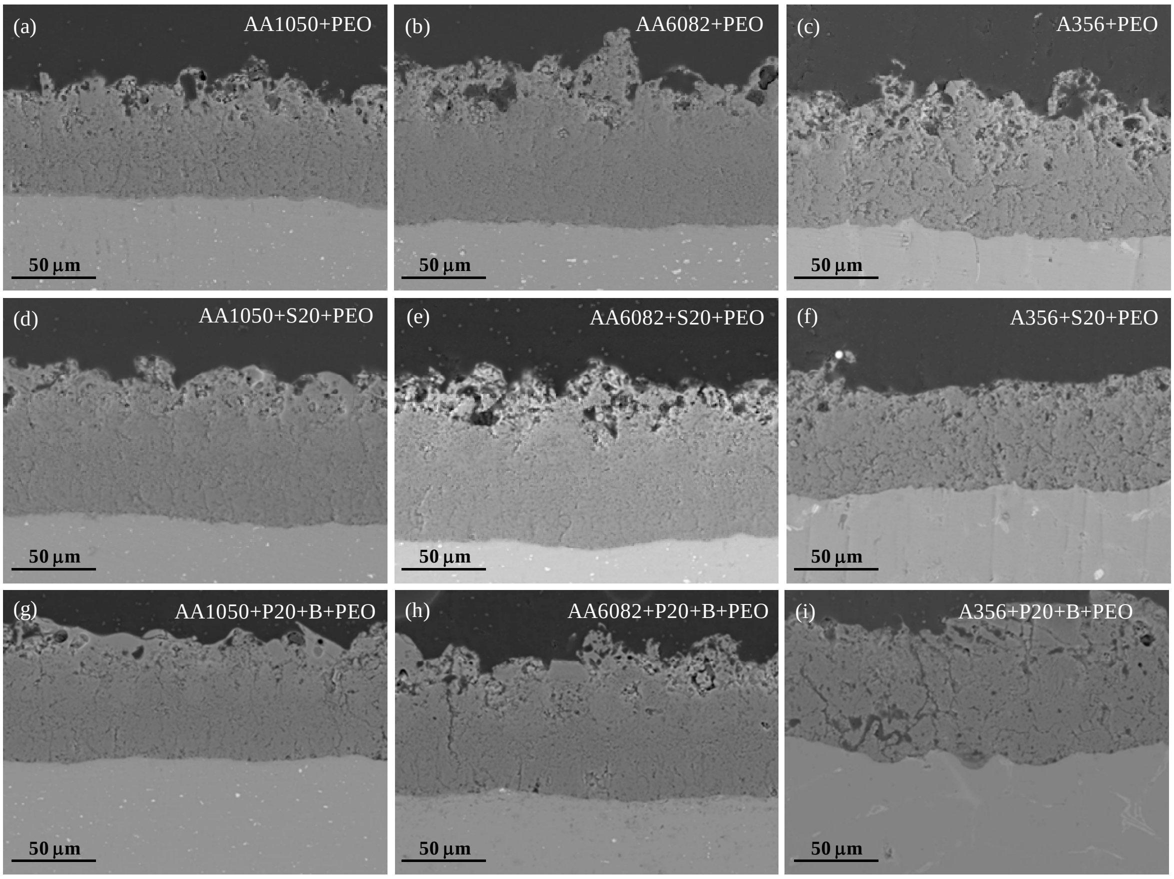

Figure 2. ***Matykina et al.***

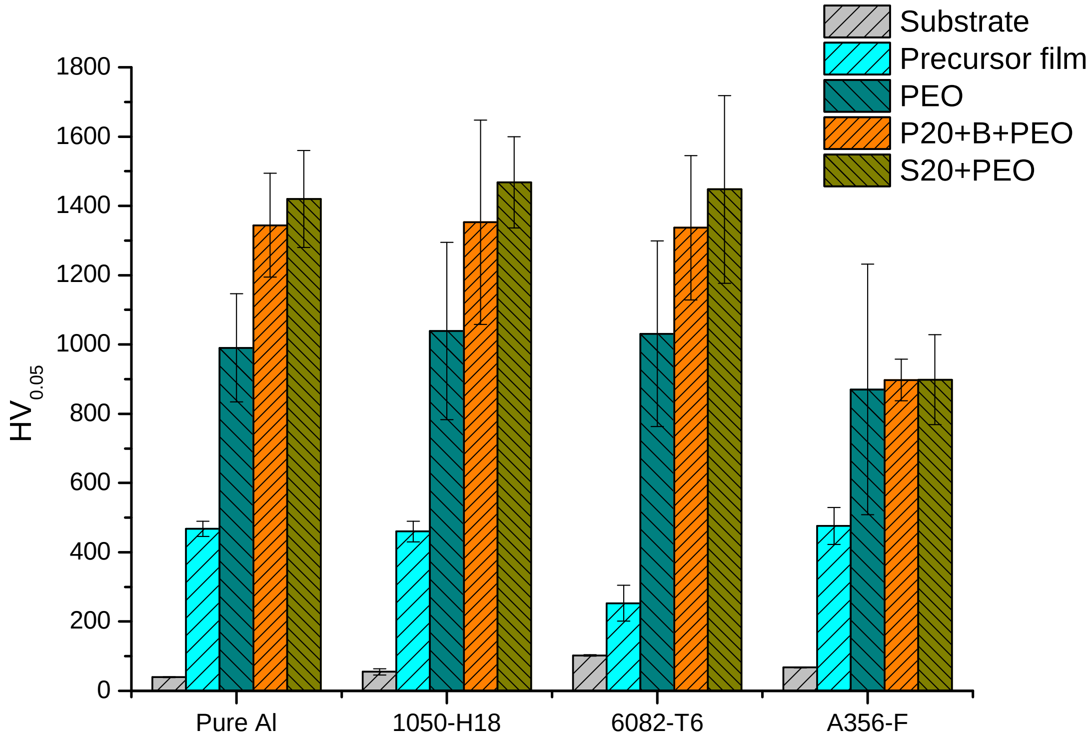

Figure 3. ***Matykina et al.***